Erschienen in: Langmuir ; 30 (2014), 42. - S. 12457-12464

Shape-Tunable Core–Shell Microparticles

Matthias K. Klein,[†] Nicolai R. Saenger,[†] Stefan Schuetter,[†] Patrick Pfleiderer,[‡] and Andreas Zumbusch*[,†]

[†]Department of Chemistry and [‡]Department of Physics,University of Konstanz, Universitätsstraße 10, 78457 Konstanz, Germany

Supporting Information

ABSTRACT: Colloidal polymer particles are an important class of materials finding use in both everyday and basic research applications. Tailoring their composition, shape, and functionality is of key importance. In this article, we describe a new class of shape tunable core–shell microparticles. They are composed of a cross linked polystyrene (PS) core and a poly(methyl methacrylate) (PMMA) shell of varying thick ness. In the first step, we prepared highly cross linked PS cores, which are subsequently transferred into a nonpolar dispersant. They serve as the seed dispersion for a nonaqueous dispersion polymerization to generate the PMMA shell. The shape of the particles can subsequently be manipulated. After the shell growth stage, the spherical PS/PMMA core–shell colloids exhibit an uneven and wrinkled surface. An additional tempering procedure allows for smoothing the surface of the core–shell colloids. This results in polymer core–shell particles with a perfectly spherical shape. In addition to this thermal smoothing of the PMMA shell, we generated a selection of shape anisotropic core–shell particles using a thermomechanical stretching procedure. Because of the unique constitution, we can selectively interrogate molecular vibrations in the PS core or the PMMA shell of the colloids using nonlinear optical microscopy techniques. This is of great interest because no photobleaching occurs, such that the particles can be tracked in real space over long times.

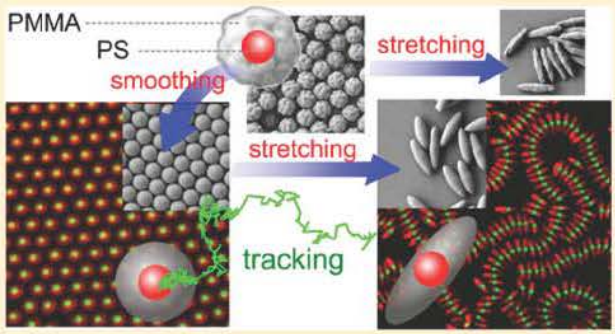

INTRODUCTION

Micrometer sized polymer particles find widespread applica tions in materials and life science and as building blocks for photonic materials.[1,2] The increasing range of applications also leads to new demands with respect to the controlled preparation of particles with specific size, functionality, and morphology. This is also true for applications in fundamental science where colloidal polymer particles are well established as model systems for the investigation of structural dynamics of atomic or molecular systems.[3−5]

Many different strategies for the preparation of polymer particles with diameters ranging from a couple of hundred nanometers to several micrometers have been developed. For the preparation of micrometer sized polymer colloids, dis persion polymerization schemes are especially well suited.[6,7] The first preparation of nonaqueous poly(methyl methacrylate) (PMMA) lattices by dispersion polymerization has been described by Osmond and Thompson.[8,9] On the basis of this scheme, Antl and co workers have developed a polymerization procedure in the presence of a presynthesized graft copolymer acting as a steric stabilizer.[10,11] Many variants of this basic procedure have been developed since then.[12−15] Examples are different kinds of fluorescently labeled and sterically stabilized PMMA particles.

Real space imaging of such model colloids using confocal fluorescence microscopy meanwhile became a widespread technique for observation.[3,4,16−18] It has motivated the preparation of a variety of different particle systems. Dullens and co workers have generated PMMA core–shell particles with fluorescently labeled cores[19,20] because this particle design allows improved localization of individual particles in dense colloidal dispersions or in the clustered state.[21−23] A problem inherent to fluorescent labeling, however, is the bleaching of the fluorescent dyes, which ultimately limits the achievable observation times for the particles. Label free coherent anti Stokes Raman scattering (CARS) microscopy[24] has therefore been presented as a promising tool for studying the dynamics of nonstained PMMA colloids on long time scales.[25] Also here, particles with core–shell morphologies would be desirable for improved localization accuracy. However, this requires core and shell materials of different chemical composition. Until now, particles of this type have not been available.

Apart from the control of the morphology of spherical polymer colloids, the control of the shape of nonspherical polymer colloids has recently generated a lot of interest.[26−30] In addition to their use as colloidal surfactants[27] or as anisotropic colloidal building blocks for the construction of hierarchical mesoscopic structures,[28,31] these systems are interesting candidates for mimicking liquid crystalline phases. One of the basic procedures for the generation of ellipsoidal polymer particles relies on the deformation of molten/liquefied polymer particles, which are embedded in a polymeric stretching

Konstanzer Online-Publikations-System (KOPS)
URL: http://nbn-resolving.de/urn:nbn:de:bsz:352-289983

matrix.[32,33] On the basis of this procedure, a multitude of differently shaped anisotropic particles has been produced.[15,26,33−35]

In this work, we report the preparation of micrometer sized core−shell particles composed of a PMMA shell and polystyrene (PS) cores, which are located in the center of the particles. For their synthesis, we combine seeded emulsion polymerization for the preparation of the cross linked PS cores[36−38] and seeded dispersion polymerization[19,20] for the subsequent growth of the PMMA shell. With this procedure, we obtain core−shell particles with a narrow size distribution. Further seeded dispersion polymerization steps increase the thickness of the final PMMA shell to the desired final particle diameter. We demonstrate that using a simple tempering procedure for the smoothing of the particles leads to nearly perfect surfaces. It is shown that the finally obtained model colloids are well suited for tracking with high contrast using CARS microscopy. In addition, we demonstrate how the thermoplastic particle shell allows for particle shaping.

EXPERIMENTAL SECTION

Materials. *Reagents for Preparing PS Particles.* Styrene, sodium dodecyl sulfate (SDS), potassium peroxodisulfate ($K_2S_2O_8$), and 1,3 diisopropenylbenzene (DIPB) were purchased from Sigma Aldrich, Germany. All reagents were used as received except for styrene, which was distilled at reduced pressure under a nitrogen atmosphere prior to polymerization. The water used for emulsion polymerization was distilled twice under nitrogen.

Reagents for PMMA Shell Synthesis. Methyl methacrylate (MMA), methacrylic acid (MA), ethyl acetate (EA), butyl acetate (BA), azo bis isobutyronitrile (AIBN), dodecane, hexane, and octyl mercaptane (OctSH) were purchased from Sigma Aldrich, Germany. MMA was purified over basic aluminum oxide (Woelm Pharma, Germany) and MA was distilled at reduced pressure to remove the respective inhibitors.

Reagents for Preparing the Stretching Film. Poly (dimethylsiloxane) ($M_n \approx 110\,000$, viscosity ≈ 50 000 cSt, PDMS), *n* hexane, methylhydrodimethyl siloxane copolymer ($M_n \approx 950$, methylhydroxysiloxane 50 mol %), and stannous 2 ethylhexanoate were purchased from Sigma Aldrich, Germany, and used as received.

Preparation of PS/PMMA Core−Shell Particles. *Synthesis of the PS Core Particles.* A three necked round bottomed flask (500 mL) equipped with a magnetic stir bar (l = 5 cm) was charged with 33.3 mg of $NaHCO_3$ (Riedel de Haën, Germany), 17.7 mg of SDS, and 350 mL of water under a nitrogen atmosphere. One milliliter of the monomer mixture (14.116 g of styrene/0.285 g of DIPB) was added, and the mixture was heated to 73 °C under stirring (500 rpm). After the polymerization temperature of 73 °C was reached, we added the initiator solution (0.102 g of $K_2S_2O_8$/10 mL of water). Thirty minutes after nucleation, the remaining monomer mixture was continuously added via a syringe pump (3.5 mL/h) over 4 h. After the completed addition, the reaction was stirred at 73 °C for an additional 20 h.

Seeded Emulsion Polymerization. The seed dispersion (0.6 mL) was added, under stirring, to 35 mL water in a 100 mL round bottomed flask with a nitrogen inlet, and the mixture was heated to 73 °C. In a second flask, we prepared a mixture consisting of 9.08 g of styrene and 0.380 g of DIPB denoted as a monomer mixture in the following text . After the addition of 1 mL of initiator solution (0.074 g of $K_2S_2O_8$ dissolved in 10 mL of H_2O), the seed dispersion was heated to 73 °C and 1.6 mL of the monomer mixture was added via a syringe pump at a rate of 0.8 mL/h. After the completed addition, the mixture was stirred for an additional 2 h at 73 °C. Finally, we filtered the dispersions through glass wool and stored them in a 50 mL centrifugation tube.

Transfer of the PS Core Dispersion into Dodecane/Hexane. To stabilize the PS cores in dodecane/hexane mixtures, we employed steric stabilizer PHSA comb PMMA. This copolymeric stabilizer consists of poly(12 hydroxystearic acid) (PHSA) chains that are linked to a PMMA backbone. The backbone is adsorbed onto the particle surface, and the PHSA chains extend into the dispersant. We prepared an ∼40% (w/w) solution of the PHSA comb PMMA copolymer in a 1:2 (w/w) BA/EA mixture according to well known procedures.[10,11,15] To prepare a stable PS core dispersion in dodecane, 8 g of the prepared PS dispersion in water was centrifuged at 3000 rpm (radius of rotor = 9.65 cm) for 20 min. After the decantation of the supernatant, we dispersed the solid residue in 5 mL of acetone (Bilgram, Germany) over 5 min. After three washing and centrifugation steps, the solid residue was mixed with approximately 5 mL of 40−60 °C petroleum ether (PE) (Sigma Aldrich). Next, we added 3 drops (0.060 g) of the steric stabilizer solution. Finally, we submerged the centrifugation tube in an ultrasonic bath and thus redispersed the particles in the PE/stabilizer mixture. The particles were washed and centrifuged twice with PE before the supernatant was decanted. For the preparation of the seed particle dispersion, the solid residue was dispersed in 0.424 g of dodecane and 0.8 g of hexane.

Seeded Dispersion Polymerization: First Growth Step. The seed particle dispersion in dodecane/hexane mixtures was mixed in a 25 mL Schlenk tube containing 0.034 g of AIBN and 8 μL of OctSH. The flask was purged with nitrogen while the oil bath was heated to 95 °C under constant stirring at 250 rpm. After reaching the desired temperature, 4.66 g of the monomer mixture composed of 10.0 g of MMA, 0.195 g of MA, 1.20 g of steric stabilizer, 7.00 g of hexane, and 3.501 g of dodecane was added at a rate of 3 mL/h. After the completed addition, the mixtures were stirred for an additional 2 h at 95 °C. After cooling to room temperature, the mixture was diluted with 5 mL of PE, filtered through glass wool, and finally transferred to a centrifuge tube. We centrifuged the resulting dispersion at 3000 rpm for 15 min. The turbid supernatant was replaced by PE and the solid residue was dispersed. The washing, dispersion, and centrifugation steps were repeated until the supernatant appeared to be clear (∼5 cycles).

Seeded Dispersion Polymerization: Second Growth Step. The dried centrifugation residue (0.713 g) obtained after the first growth step was dispersed in 0.3 g of dodecane and 0.6 g of hexane. The dispersion was mixed with 0.036 g of AIBN and 8 μL of OctSH. The mixture was heated to 95 °C under a flow of nitrogen. We continuously added 5.12 g of the monomer mixture, already used for the first growth step, over 2 h. After an additional 1.5 h of stirring, the particle dispersion was cleaned as described in the previous section.

Thermal Smoothing of the Particle Surface. Particle samples were dispersed in decalin, amounting to total mass contents of between 5 and 25% (w/w). To prevent oxidation leading to colloidal instability, we purged the respective dispersions with nitrogen for 10 min under stirring. After the colloids were heated to 160 °C, we stirred them at this temperature for 1 h. This procedure led to a considerable smoothing of the particle surface.

Particle Stretching. We embedded the different particle samples in cross linked PDMS films (details given in the SI). After the curing step, we cut the film into 2 cm wide stripes, which we subsequently fixed between two movable sets of clamps. The whole assembly was heated to 165 °C. Afterward, the films were stretched at this temperature by factors of 1.5, 2.3, and 3.0. After cooling, the films were degraded for 18 h. The degrading mixture was prepared such that it was composed of 3.47% PDMS film, 78.81% hexane, 17.72% isopropanol, and 0.04% sodium methoxide by weight. The released particles were washed with the hexane/isopropanol mixture and finally restabilized with a mixture composed of 5 parts decalin and 1 part EA/BA mixture (2:1 w/w) containing 1% w/w steric stabilizer.

Sample Preparation for Optical Microscopy. *General Procedure.* To prepare samples for optical microscopy, approximately 5 μL of each colloidal dispersion was spread on microscope coverslips. In the case of aqueous PS core dispersions, the coverslip was previously exposed to oxygen plasma in order to increase the hydrophilicity. After the evaporation of the dispersant, the samples were either measured in air or covered with immersion oil.

Sample Preparation for CARS Tracking Experiments. The dispersion was adjusted to a volume fraction ϕ_v of 0.4 and used to fill a glass capillary (0.20 mm × 4.00 mm; CM Scientific, U.K.), which was subsequently sealed with an UV curable glue (optical adhesive, Norland, USA).

Analytical Methods. *Dynamic Light Scattering.* Dynamic light scattering (DLS) was performed on a Malvern Nano ZS ZEN 3600 particle sizer (173° backscattering geometry, Malvern, U.K.). The autocorrelation function was analyzed using the Malvern dispersion technology software 5.10 algorithm to retrieve the volume and number average particle size distributions of the PS seed particles. Samples were prepared by diluting 5 μL of each dispersion with approximately 3 mL of water.

Electron Microscopy. Scanning electron microscopy (SEM) was conducted on a CrossBeam 1540XB (Carl Zeiss, Germany). For SEM measurements, we dried the dilute particle dispersions on silicon wafers and sputter coated the samples with 5 nm thick gold layers. Images were recorded using a secondary electron detector at an acceleration voltage of 1 kV. The particle analyzer plugin of ImageJ was used to retrieve particle diameters from SEM and TEM images.

Differential Interference Contrast (DIC) Microscopy. Differential interference contrast (DIC) images were recorded on a Leica DMI 6000B microscope using a 100×/1.4−0.7 oil immersion CS objective (Leica Microsystems, Germany).

CARS Microscopy. For CARS microscopy experiments, we used a home built setup based on a Leica TCS SP5 multiphoton microscope (Leica Microsystems, Germany). A Nd:YVO_4 laser delivering 7 ps pulses at a repetition rate of 76 MHz and a wavelength of 532 nm (HighQ, Austria) was used to pump an optical parametric oscillator (APE, Germany), the signal beam of which was used as a pump beam. Imaging of the PS cores and the complete colloids was performed at pump wavelengths of 809.6 and 803.2 nm corresponding to vibrational frequencies of 3052 and 2953 cm^{-1}, respectively. We used a Leica 1.2 NA, 63× water immersion objective for imaging (Leica Microsystems, Germany). The respective CARS signals of the PS cores or the PMMA shells, located at 653 and 645 nm, were collected in the forward direction by a condenser lens, selected using band pass filters, and detected with a photomultiplier tube. Volume scans of individual particles were generated by raster scanning the samples in three dimensions.

RESULTS AND DISCUSSION

As detailed above, our aim was the development of a core−shell microparticle system that is suited for high precision localization microscopy and can be brought into nonspherical shape in a controlled fashion. We therefore prepared particles composed of micrometer sized PS cores, which are covered with a PMMA shell. This particle morphology offers the possibility to engineer the particle shape and surface without affecting the shape of the cross linked, spherical PS centers. We chose PS microgel colloids as the core material because of the aromatic groups of the polymer network. Because the PMMA shell is purely aliphatic, one can visualize the chemical contrast between the core and shell materials. Therefore, the system is suitable for the selective imaging of either individual particle cores or entire colloids with CARS microscopy.

Preparation of the Core−Shell Colloids. To prepare core−shell colloids of the type described, we first generated cross linked PS seeds with a diameter of 280 nm via emulsion polymerization. Their number average mean diameter was retrieved from DLS measurements (SI). The final PS cores with the desired diameter of ~875 nm were obtained after a further seeded emulsion polymerization step (Figure 1, histrogram (black distribution)). Concerning the PS core latex, the slow and undisturbed evaporation of water at ambient temperature (22 °C) yielded expanded 2D colloidal crystals. The colloidal crystallites exhibited radiant colors depending on the angle of

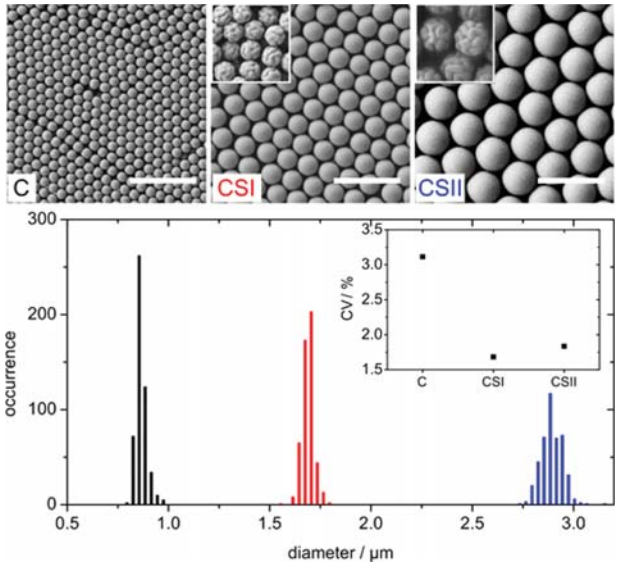

Figure 1. SEM micrographs and size distributions of the colloids after different polymerization stages. C, CSI, and CSII correspond to PS cores and core−shell particles after the first (I) and second (II) growth stages of the PMMA shell, respectively, after surface smoothing. Insets show the particles before surface smoothing. Scale bars: 5 μm. The histogram depicts the size distributions of each particle population retrieved from the SEM images. The inset shows the corresponding CV values.

incident light due to Bragg diffraction.[39] To perform non aqueous seeded dispersion polymerization, we transferred these PS core particles as synthesized into a mixture consisting of aliphatic hydrocarbons. The PMMA shell was grown on the sterically stabilized PS cores in two subsequent seeded dispersion polymerization steps (indicated as I and II in particle denotations). We found that the degree of cross linking in the PS core particles was a crucial parameter for the transfer of the PS particles into the desired aliphatic hydrocarbon mixture in the dispersed, nonaggregated state. In this step, low cross linker contents in the PS microgel particles lead to flocculation of the colloids when washing with acetone. In the case of higher cross linker contents, we observed stable dispersions in acetone without any signs of flocculation. After replacing the acetone with PE and the steric stabilizer was adsorbed[10,15] during ultrasonication, stable PS dispersions in dodecane/hexane mixtures were obtained. In the following text, the resulting PS dispersions served as seed dispersions for the subsequent seeded dispersion polymerization. Despite the delayed and slow addition of the monomer mixture during the seeded dispersion polymerization, which is necessary to guarantee starved feeding conditions, we could not completely avoid the formation of secondary nucleated particles. However, because of the pronounced size difference between the two particle species, the two different particle fractions are easily separable by centrifugation. Adjusting the number of PS core particles and the mass of the added monomer mixture allows for an estimation of the final particle diameters. After the removal of secondary nucleated particles and the surface smoothing procedure, which will be explained later, we imaged the colloids after the different steps of the colloid preparation using scanning electron microscopy (SEM, Figure 1, upper row). Before surface smoothing, the core−shell particles showed a rough and wrinkled surface (Figure 1, SEM image

insets). This was already reported by other groups for the synthesis of cross linked core−shell particle systems.[20,21] To evaluate individual size distributions, we extracted the diameters of several hundred particles from the SEM images. In addition, we calculated the coefficient of variation (CV) for the particle diameters at each stage by considering between 442 and 509 particle diameters.[40] In the bottom part of Figure 1, particle size distributions retrieved from SEM micrographs are depicted. The black distribution in Figure 1 belongs to the PS core particles (C). The distribution, highlighted in red, represents the smoothed core−shell particles after the first growth stage (CSIs). The distribution obtained for the particles after the second growth stage and subsequent surface smoothing (CSIIs) is marked in blue. Details about the image processing and data analysis are provided in the SI. We finally obtained particles with mean diameters of 1.7 and 2.9 μm for CSIs and CSIIs, respectively. One can note the rather narrow size distributions after each step of the colloid preparation. The inset of the histogram (Figure 1) shows the development of the CV values after the subsequent growth stages and surface smoothing. The CV of individual particle populations drops from 3.1% for C to 1.7% for CSIs and slightly increases to 1.8% for CSIIs.

The synthesis of the particles just described offers a lot of flexibility for the introduction of specific functions. Except for the particles having fluorescent PS cores, which are presented in the SI, we prepared the core−shell particles without any cross linker in the PMMA shell. This is a crucial requirement for the further thermomechanical deformation of the shell. Additionally, this offers the possibility to smooth the surface of the core−shell colloids, as will be explained in the following section. The simplest method for the investigation of the core−shell morphology of the colloids is the covering of particle layers with microscopy immersion oil. This adjusts the refractive index of the surrounding medium to that of PMMA (n_D = 1.4914)[41] and nicely reveals the core−shell structure. Figure 2 depicts dried layers of CSIIr (Figure 2A) and CSIIs (Figure 2C) as prepared (with *r* indicating the rough, unsmoothed surface) and the same areas in immersion oil (Figure 2B,D). As expected, the PMMA shells are perceptible only in air whereas the spherical PS cores with a refractive index close to 1.54 become visible when the particles are covered with immersion oil.

Tempering Procedure. To liquefy the shell polymer, we heated the colloids (CSIr and CSIIr) dispersed in decalin to above the glass transition temperature (T_g) of the PMMA. The spherical geometry has the smallest surface area for a given volume. Therefore, the tendency to reduce the surface energy in combination with the increased polymer chain mobility in the particle shells above T_g leads to an efficient smoothing of the particles' surfaces. Besides surface smoothing, we also observed particle coalescence of two or more particles, which are fusing to one larger particle. We could separate the fraction of fused particles by sedimentation as a result of their larger sphere diameters, which scale with $n^{1/3}$ (with *n* being the number of fused core−shell particles). After 1 h of stirring at 160 °C, the colloids and the resulting clusters appeared to be ideal microspheres (Figure 1, SEM images). Interestingly, despite the embedded strongly anisotropic PS core clusters, as for example observed for clusters containing two PS cores, the outer shape of the core−shell clusters stays spherical. Only larger clusters containing more than four cores significantly deviate from the spherical shape. Because these clusters represent an interesting class of colloids on their own, their isolation, purification, and application will be the object of another article. For many experiments, it is desirable to covalently link the stabilizer backbone to the particle surface. Usually, this can be achieved by reacting the carboxyl groups on the particle surface with the epoxy functionalities of the stabilizer backbone to ester linkages. Despite the absence of a ring opening catalyst, which would facilitate this reaction, the stabilizer seems to have covalently linked during the tempering process. We come to this conclusion because the particles maintain their colloidal stability even after several washing and centrifugation steps in decalin and/or CHB. At this point, we want to emphasize that the tempering procedure is a powerful tool for rendering many kinds of non cross linked, surface structured PMMA colloids as ideal microspheres.

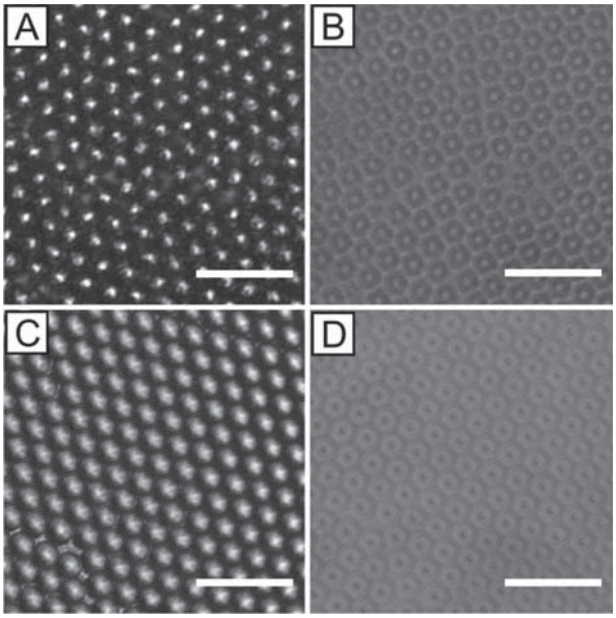

Figure 2. Transmitted light microscopy images of different core−shell particles in air and in immersion oil. (A, B) CSIIr and (C, D) CSIIs observed (A, C) in air or (B, D) in an oil immersion where the PMMA shells are nearly refractive index matched. Scale bars: 10 μm.

Thermomechanical Stretching of Core−Shell Colloids. In the following text, we used the core−shell colloids as precursors for the production of shape anisotropic particles. Thus, we subjected the spherical core−shell colloids to the thermomechanic stretching procedure, which has initially been reported by Keller and co workers.[32] With this method, we could produce large amounts (up to several grams) of shape anisotropic particles. In the first step, the CSI colloids were embedded in a stretching matrix composed of cross linked PDMS. After the particle laden stripes were heated to above the T_g of the PMMA shell, the films were stretched by factors of x = 1.5, 2.3 and 3.0 in a self made stretching apparatus. We thermomechanically stretched both the rough and smoothed core−shell CSIr and CSIs particles. Details about the workflow are given in the SI. As illustrated in Figure 3, the stretching of the rough precursor particles (Figure 3A) resulted in rough ellipsoids (Figure 3C,E,G). Similarly, smoothed, spherical particles (Figure 3B) lead to ellipsoids with a smooth surface (Figure 3D,F,H). This results from the nearly affine stretching procedure. The stretching matrix forms a replica of the surface topography of individual particles as already postulated by

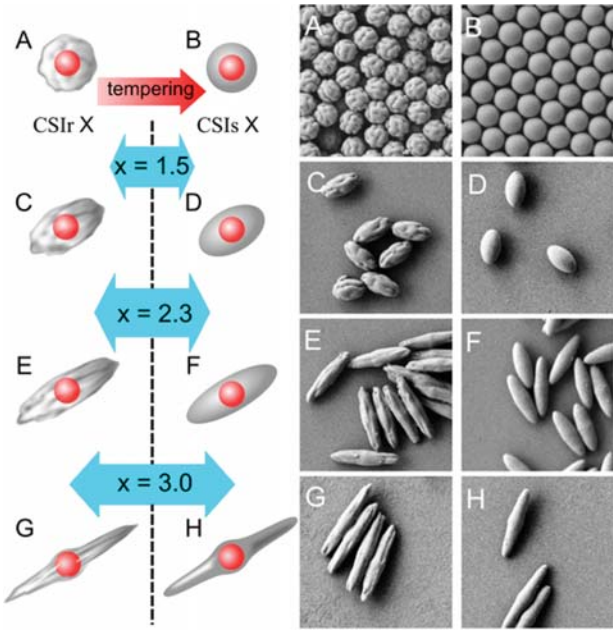

Figure 3. Thermomechanical deformation of core−shell colloids. (Left) Schematic illustration of particle stretching using rough (CSIr) (A, C, E, G) or smoothed (CSIs) precursors (B, D, F, H), with x indicating the stretching factor. (Right) SEM images. The dimensions of the images correspond to 10 μm × 10 μm.

Keville et al.[42] During stretching, this replica is deformed along the stretching direction and the polymer melt completely fills this elongated micromold. After cooling, this finally leads to surface structured anisotropic particles. Therefore, the possibility to smooth the surface of the spherical precursors allows for the production of core−shell ellipsoids with either smooth or wrinkled surfaces. This transformation of the surface features depends on the feature size and the flexibility of the embedding matrix. We expect that there is a lower size limit for the surface features, which can be shape transformed. Concerning the wrinkles in our colloids, this mold stretching assumption seems to be appropriate. However, the resulting shape after stretching is additionally dictated by the diameter of the embedded, cross linked PS core. The core diameter limits the thinning of the particle waist during particle deformation. Employing stretching factors larger than 2.3, we observed elongated particles with bulgy waists and sharp tips (Figure 3G,H).

In all particle samples, we observed spherical PS cores in the final deformed colloids. They were not affected by the stretching procedure because of their high degree of cross linking, which precludes permanent deformation.[42] After the thermomechanical stretching, the particles were released by degrading the stretching matrix. In total, we prepared six different batches of thermomechanically deformed core−shell particles. After stretching and release, the different particle batches were restabilized and redispersed in decalin.

CARS Microscopy. We chose the PS/PMMA system because, although it exhibits different chemical structures, it still shows comparable densities. We exploited the difference in the chemical nature of colloid cores and shells for generating particle images using CARS microscopy.[24] The aromatic CH stretching vibrational frequencies are spectrally well separated from the aliphatic CH resonances of the PMMA shell and aliphatic dispersants *cis*/*trans* decalin and cyclohexylbromid (CHB).[25] It is therefore possible to image the particle cores at high contrast, which in turn is the basis for the determination of the particle positions with high accuracy.

Confocal CARS microscopy allows imaging with a lateral resolution of 0.4 μm × 0.4 μm and an axial resolution of ∼1.2 μm. Typical excitation powers of the pump and Stokes laser were 70 and 30 mW, respectively. Because of the long wavelengths used for coherent excitation, compared to confocal fluorescence microscopy, using Rhodamine B as a fluorescent label, scattering is significantly reduced. This is a striking advantage for imaging deep inside colloidal dispersions, as will be detailed below. Because we intensely washed the PS cores prior to shell growth, we reliably extracted residual non cross linked PS. This leads to precisely defined particle cores, clearly separated from the shell region of the particle. The distinct separation of the core and shell region could also be confirmed for core−shell particles prepared starting from fluorescently stained PS cores (SI).

As a first experiment, we imaged colloidal crystalline monolayers composed of CSIIs spherical core−shell particles using CARS microscopy. In these samples composed of dried particle layers on microscope slides, we could selectively image either the PS cores (green channel) or the complete colloids (red channel) as illustrated in Figure 4A,B. The resulting merging of both channels is displayed in Figure 4C. For image acquisition, we tuned the frequency of the Stokes beam ν_s such that the energy difference $\nu_p - \nu_s$ between the Stokes and pump (ν_p) beams matches the corresponding vibrational frequency ν_{vib}. To demonstrate the chemical selectivity, we depict a colloidal crystalline area containing one PMMA particle lacking a PS core. When imaged at a PS resonance frequency, this particle, marked by the white square in Figure

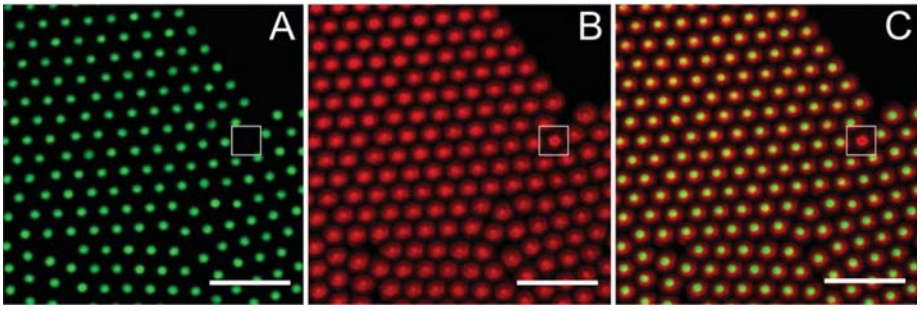

Figure 4. CARS imaging of spherical core−shell colloids. (A−C) Colloidal crystalline monolayer of CSIIs imaged at the (A) aromatic and (B) aliphatic resonance frequencies with (C) the resulting merge. PMMA colloid with PS core lacking is indicated by the white square. Scale bars: 10 μm.

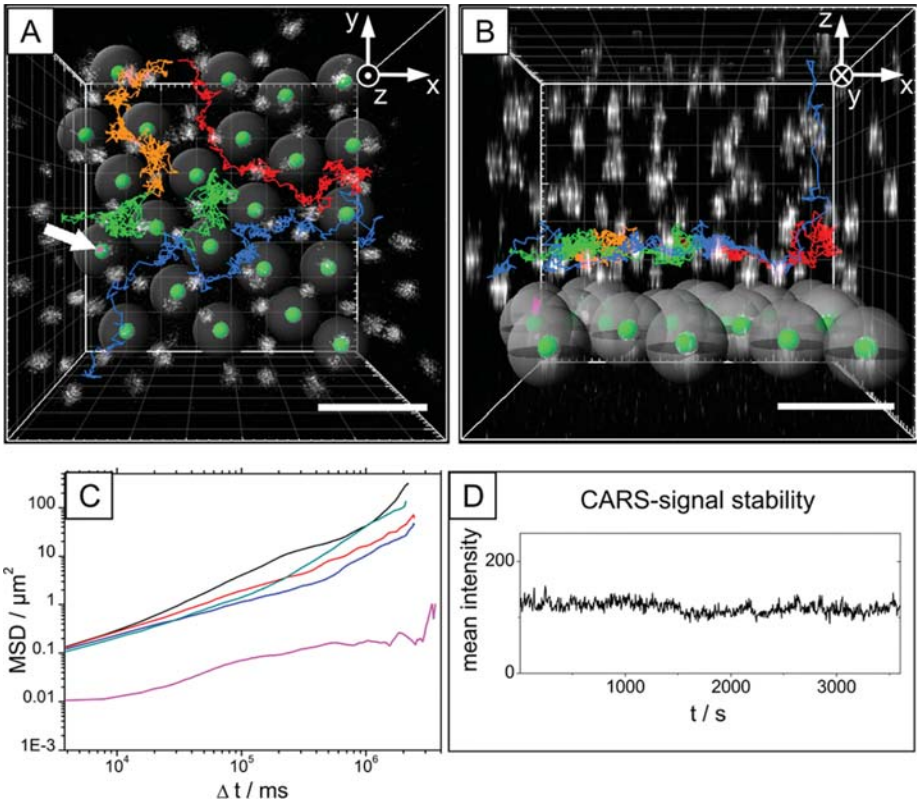

Figure 5. Long term CARS single particle tracking of CSIIs colloids in a dense dispersion. Four dimensional series of core−shell particles were acquired during 1 h at the aromatic resonance frequency of $\nu_p - \nu_s$ = 3052 cm^{-1} (7.7 fps, 0.25 stacks/s). (A) First volume scan overlaid with the subsequent trajectories of representative particles with the line of vision along the z axis. (B) Image of the same volume scan with the viewing direction along the y axis (A). The CARS signal corresponds to the colloid cores displayed in grayscale. For the particles at the glass surface, the core and the shell are indicated as green and translucent gray spheres, respectively. The white arrow highlights the otherwise not very visible trajectory. Scale bars: 5 μm. (C) MSD plots of the trajectories visible in A and B identified by the color coding. (D) Intensity−time profile of the core signal highlighted with the white arrow in A. In the case of fluorescent labeling, the signal would decay significantly.

4A−C, gives no signal (Figure 4 A) whereas the cores of the neighboring particles remain visible.

In the second experiment, we demonstrate the long term traceability of single core−shell particles in dense dispersions via CARS microscopy. For this purpose, we prepared dispersions of the core−shell colloids in a density matching mixture consisting of cyclohexylbromide and decalin (85:15 w/w). Because the estimated mass density of the CSIIs particles is only ~0.3% smaller than that of common PMMA particles, we neglected this deviation in the following experiments. For the investigated sample, we chose a volume fraction ϕ_v of 0.4, which is well below the value of 0.58 defining the colloidal glass transition of sterically stabilized colloids.[3,17,18] Three dimensional imaging was performed at $\nu_p - \nu_s$ = 3052 cm^{-1}, matching the vibrational frequency of the PS cores. Diffusive single particle movement in dispersion was followed by sampling a volume of 15.5 μm × 15.5 μm × 14.7 μm at a frequency of 0.255 Hz for 1 h. To analyze the 3D particle movement, we used the commercial tracking software Imaris (version 7.6.0, Bitplane). To the analysis, the software rendered the CARS signal, originating from individual PS cores, with green spheres (Figure 5A,B). For generate a picture of whole colloids, translucent gray spheres were drawn to visualize the space occupied by the PMMA shells.

The center coordinates of the particles were detected for each volume scan in order to reconstruct individual particle trajectories. The sampled volume was selected such that we could observe mobile and immobile particles. The first imaged layer comprises immobile particles, which are adsorbed on the glass surface of the capillary (Figure 5A,B, pink trajectory). Because all of these bottom particles show the same collective motion, we attribute this distinct movement to a slight drift in the sample during the measurement. Because these bottom particles are immobilized on the glass surface, they show the lowest displacement over time. In the subsequent particle layer, we tracked colloids showing a larger displacement, which, however, are still influenced by the bottom layer (Figure 5A,B, green and orange trajectory). At higher sampling depths, we observed the largest mobility of individual particles (Figure 5A,B, red and blue trajectories). These particles were usually crossing the entire sampled volume within the course of the measurement. With this particle system and imaging technique, we can follow individual particle trajectories with high temporal and spatial resolution. Figure 5C shows the development of the mean square displacement (MSD) over time. For clarity, we solely considered the blue, green, orange, red, and pink trajectories visible in Figure 5A.[43] Using the Stokes−Einstein formula, we calculated individual diffusion coefficients from the respective MSD plots using linear fitting. For mobile particles, we determined diffusion coefficient ranging from 1.06 × 10^{-3} to 5.8 × 10^{-3} μm^2 s^{-1}. Additionally, we show the mean signal intensity during the course of measurement (Figure 5D),

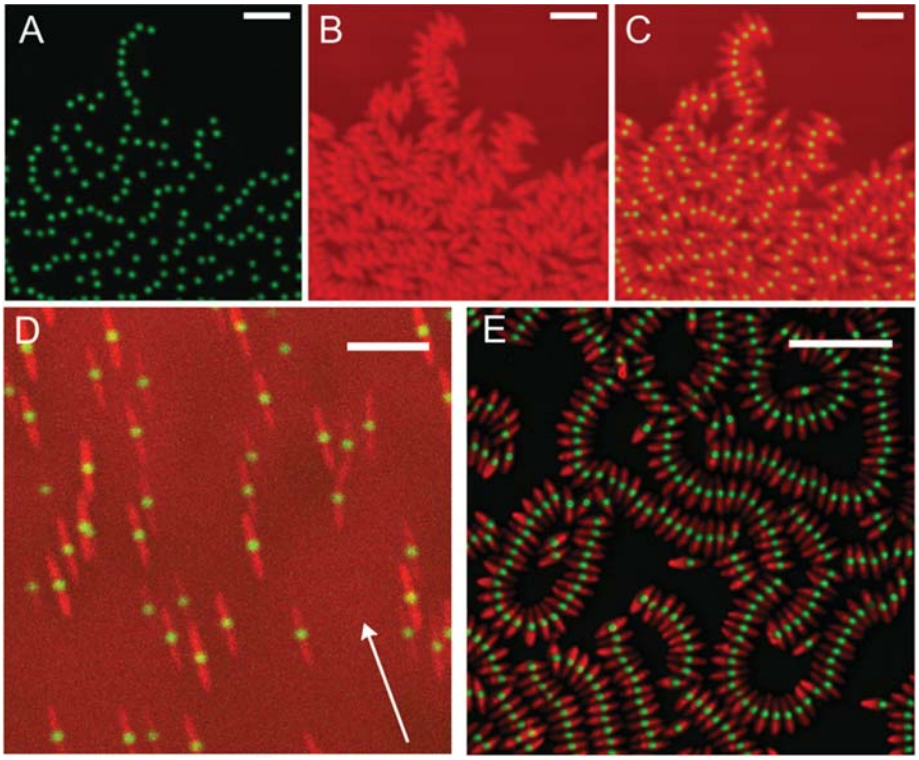

Figure 6. CARS images of representative core−shell particle samples imaged at the aromatic (green) and aliphatic (red) resonance frequency. For clarity, the two imaging frequencies are merged (C, E). (A−C) Anisotropic colloids CSIs2.3 dispersed in decalin. Note that image E was acquired at $\nu_p - \nu_s = 2845\ cm^{-1}$ and the signal has been inverted.[25] (D) Ellipsoids still embedded in the PDMS film (maximum projection). The white arrow indicates the stretching direction. Scale bar: 5 μm. (E) CSIs2.3 chainlike, organized, dried ellipsoids. Scale bar: 10 μm.

highlighting the temporal stability of the CARS signal. This underlines that this approach is well suited for long term measurements because in contrast to fluorescence microscopy based approaches no photobleaching occurs. The entire movie of the tracking experiment is provided as Supporting Information. Despite the scattering on the PS cores, which are compared to the PMMA shells not index matched, we could image particle cores at measurement depths of up to ∼85 μm from the surface of the capillary (SI). In this case, the signal intensity benefits from reduced scattering resulting from the long wavelength excitation and emission. Hence, with this particle system and the employed CARS imaging technique we can also image individual particles deep inside a dense dispersion because it is necessary to exclude wall effects.[3,4,25]

Finally, CARS microscopy was also used as an analytical tool to confirm individual particle morphologies after the afore mentioned thermomechanical shell deformation. As already demonstrated for the CSIIs spherical particles, with CARS microscopy we can distinguish between the PS core and the entire particle volume. Right after the deformation of the colloid shell, we imaged the CSIr2.3 colloids, still embedded in the stretching film (Figure 6D). Even in this case, where aliphatic CH stretching vibrations of the PDMS matrix generate a considerable background, one can clearly distinguish the ellipsoids, which are aligned along the stretching direction. The stretching direction is indicated by the white arrow.

Images recorded at the aromatic CH resonance of polystyrene, located at $\nu_p - \nu_s = 3052\ cm^{-1}$, reveal the random distribution of individual particle centers (Figure 6D). Because of the absence of aromatic functionalities in the surrounding stretching matrix, the signal to background ratio significantly increases by a factor of ∼3 compared to the value obtained for the aliphatic resonance frequency.

After film degradation and restabilization[28] of the isolated ellipsoids, we generated dispersions of the respective colloids in decalin. Figure 6A−C shows ellipsoids on the bottom of the sample chamber. In this case, we also observed a significant increase in the signal to background ratio at the PS resonance frequency (Figure 6 A) compared to the aliphatic channel (Figure 6B). The CSIs2.3 particles showed a strong tendency to organize into chainlike structures upon dispersant evaporation. In this case, we could also selectively image either the particle cores or the entire particle. As depicted in Figure 6E, imaging at the resonance frequency of the PS cores clearly reveals the chainlike alignment of the shape anisotropic colloids. This is one example, chosen from a multitude of mesoscopic hierarchical structures, that can be assembled using these anisotropic core−shell colloids as colloidal building units. Depending on the refractive index of their environment, the optical properties of such structures can be modulated.[44]

■ CONCLUSIONS

We have introduced a PS/PMMA core−shell particle system derived from state of the art, sterically stabilized PMMA colloids. Because of the chosen polymers, we can selectively image the particle cores or the entire colloid volume using CARS microscopy. We demonstrate how the movement of individual colloids in dispersion can be followed over long time scales, which points to their potential application as colloidal model system. Because of their core−shell morphology, this

particle system allows for high contrast 4D particle tracking even in dense dispersions. Additionally, we demonstrate the manifold possibilities of postengineering the particle shell. As an example, we liquefied the wrinkled particle shell to generate ideal core−shell microspheres. Starting from differently surface structured, spherical core−shell particles, we generated differently shaped anisotropic core−shell particles. In each case, despite the deformation of the thermoplastic PMMA shell, the cross linked PS cores stay spherical. In a forthcoming manuscript, we will especially focus on the hydrodynamics of the ellipsoidal core−shell colloids as already analyzed for other kinds of anisotropic colloids.[45−47] We want to emphasize that this particle system is appealing for many other applications, especially for optical tweezing experiments, where the particles could be optically manipulated under refractive index matching conditions in mixtures with common PMMA particles.

■ ASSOCIATED CONTENT

● Supporting Information

Preparation of CS particles with fluorescent cores. Retrieval of particle size distributions from SEM images. Details of the thermomechanical stretching procedure. Video of the CARS tracking experiment. This material is available free of charge via the Internet at http://pubs.acs.org.

■ AUTHOR INFORMATION

Corresponding Author

*Fax: +49 7531 88 3139. Phone: +49 7531 88 2357. E mail: andreas.zumbusch@uni konstanz.de.

Author Contributions

The manuscript was written through the contributions of all authors. All authors have given approval to the final version of the manuscript.

Notes

The authors declare no competing financial interest.

■ ACKNOWLEDGMENTS

We gratefully acknowledge C. Rosazza and A. Buntz for support concerning particle tracking and MSD analysis as well as fruitful discussions. Additionally, we thank R. Görgülü for assistance concerning CARS measurements.

■ REFERENCES

(1) Lu, Y.; Yin, Y. D.; Xia, Y. N. *Adv. Mater.* **2001**, *13*, 415−420.
(2) Kim, S. H.; Park, H. S.; Choi, J. H.; Shim, J. W.; Yang, S. M. *Adv. Mater.* **2010**, *22*, 946−950.
(3) Weeks, E. R.; Crocker, J. C.; Levitt, A. C.; Schofield, A.; Weitz, D. A. *Science* **2000**, *287*, 627−631.
(4) Gasser, U.; Weeks, E. R.; Schofield, A.; Pusey, P. N.; Weitz, D. A. *Science* **2001**, *292*, 258−262.
(5) Martelozzo, V. C.; Schofield, A. B.; Poon, W. C. K.; Pusey, P. N. *Phys. Rev. E* **2002**, *66*, 021408.
(6) Song, J. S.; Tronc, F.; Winnik, M. A. *Polymer* **2006**, *47*, 817−825.
(7) Campbell, A. I.; Bartlett, P. *J. Colloid Interface Sci.* **2002**, *256*, 325−330.
(8) Osmond, D. W. J.; Thompson, H. H. Dispersion Polymerization. British Patent GB893429, 1962.
(9) Barrett, K. E. J., Ed. *Dispersion Polymerization in Organic Media*; Wiley: London, 1974.
(10) Antl, L.; Goodwin, J. W.; Hill, R. D.; Ottewill, R. H.; Owens, S. M.; Papworth, S.; Waters, J. A. *Colloids Surf.* **1986**, *17*, 67−78.
(11) Elsesser, M. T.; Hollingsworth, A. D. *Langmuir* **2010**, *26*, 17989−17996.
(12) Bosma, G.; Pathmamanoharan, C.; de Hoog, E. H.; Kegel, W. K.; van Blaaderen, A.; Lekkerkerker, H. N. *J. Colloid Interface Sci.* **2002**, *245*, 292−300.
(13) Dullens, R. P. A.; Claesson, E. M.; Kegel, W. K. *Langmuir* **2004**, *20*, 658−664.
(14) Hu, H.; Larson, R. G. *Langmuir* **2004**, *20*, 7436−7443.
(15) Klein, M. K.; Zumbusch, A.; Pfleiderer, P. *J. Mater. Chem. C* **2013**, *1*, 7228−7236.
(16) Dinsmore, A. D.; Weeks, E. R.; Prasad, V.; Levitt, A. C.; Weitz, D. A. *Appl. Opt.* **2001**, *40*, 4152−4159.
(17) Poon, W. C. K.; Weeks, E. R.; Royall, C. P. *Soft Matter* **2012**, *8*, 21−30.
(18) Royall, C. P.; Poon, W. C. K.; Weeks, E. R. *Soft Matter* **2013**, *9*, 17−27.
(19) Dullens, R. P. A. *Soft Matter* **2006**, *2*, 805−810.
(20) Dullens, R. P. A.; Claesson, M.; Derks, D.; van Blaaderen, A.; Kegel, W. K. *Langmuir* **2003**, *19*, 5963−5966.
(21) Elsesser, M. T.; Hollingsworth, A. D.; Edmond, K. V.; Pine, D. J. *Langmuir* **2011**, *27*, 917−927.
(22) Crassous, J. J.; Dietsch, H.; Pfleiderer, P.; Malik, V.; Diaz, A.; Hirshi, L. A.; Drechsler, M.; Schurtenberger, P. *Soft Matter* **2012**, *8*, 3538−3548.
(23) Schneider, D.; Beltramo, P. J.; Mattarelli, M.; Pfleiderer, P.; Vermant, J.; Crespy, D.; Montagna, M.; Furst, E. M.; Fytas, G. *Soft Matter* **2013**, *9*, 9129−9136.
(24) Zumbusch, A.; Holtom, G. R.; Xie, X. S. *Phys. Rev. Lett.* **1999**, *82*, 4142−4145.
(25) Kaufman, L. J.; Weitz, D. A. *J. Chem. Phys.* **2006**, *125*, 074716.
(26) Liu, B.; Wang, D. Y. *Langmuir* **2012**, *28*, 6436−6440.
(27) Kim, J. W.; Larsen, R. J.; Weitz, D. A. *J. Am. Chem. Soc.* **2006**, *128*, 14374−14377.
(28) Zhang, Z. K.; Pfleiderer, P.; Schofield, A. B.; Clasen, C.; Vermant, J. *J. Am. Chem. Soc.* **2011**, *133*, 392−395.
(29) Hu, Y. D.; Wang, Q.; Wang, J. Y.; Zhu, J. T.; Wang, H.; Yang, Y. J. *Biomicrofluidics* **2012**, *6*, 026502.
(30) Nagao, D.; Hashimoto, M.; Hayasaka, K.; Konno, M. *Macromol. Rapid Commun.* **2008**, *29*, 1484−1488.
(31) Glotzer, S. C.; Solomon, M. J. *Nat. Mater.* **2007**, *6*, 557−562.
(32) Ho, C. C.; Keller, A.; Odell, J. A.; Ottewill, R. H. *Polym. Int.* **1993**, *30*, 207−211.
(33) Mohraz, A.; Solomon, M. J. *Langmuir* **2005**, *21*, 5298−5306.
(34) Champion, J. A.; Katare, Y. K.; Mitragotri, S. *Proc. Natl. Acad. Sci. U.S.A.* **2007**, *104*, 11901−11904.
(35) Fernandez Nieves, A.; Cristobal, G.; Garces Chavez, V.; Spalding, G. C.; Dholakia, K.; Weitz, D. A. *Adv. Mater.* **2005**, *17*, 680−684.
(36) Vanderhoff, B. M. E. *J. Polym. Sci.* **1960**, *48*, 175−188.
(37) Vanderhoff, B. M. E. *J. Polym. Sci.* **1960**, *44*, 241−259.
(38) Zillessen, A.; Bartsch, E. *Langmuir* **2009**, *26*, 89−96.
(39) Krieger, I. M.; Oneill, F. M. *J. Am. Chem. Soc.* **1968**, *90*, 3114−3120.
(40) Ha, S. T.; Park, O. O.; Im, S. H. *Macromol. Res.* **2010**, *18*, 935−943.
(41) Mark, J. E. *Polymer Data Handbook*; Oxford University Press: New York, 1999.
(42) Keville, K. M.; Franses, E. I.; Caruthers, J. M. *J. Colloid Interface Sci.* **1991**, *144*, 103−126.
(43) Tinevez, J. Y. *Mean Square Displacement Analysis of Particles Trajectories*; MATLAB class, 2013.
(44) Sherman, R. L.; Ford, W. T. *Ind. Eng. Chem. Res.* **2005**, *44*, 8538−8541.
(45) Han, Y.; Alsayed, A. M.; Nobili, M.; Zhang, J.; Lubensky, T. C.; Yodh, A. G. *Science* **2006**, *314*, 626−630.
(46) Martchenko, I.; Dietsch, H.; Moitzi, C.; Schurtenberger, P. *J. Phys. Chem. B* **2011**, *115*, 14838−14845.
(47) Reddy, N. K.; Perez Juste, J.; Pastoriza Santos, I.; Lang, P. R.; Dhont, J. K. G.; Liz Marzan, L. M.; Vermant, J. *ACS Nano* **2011**, *5*, 4935−4944.